JOURNAL OF MATERIALS SCIENCE 27 (1992) 319–327

Electrochemical deposition of polypyrrole on carbon fibres for improved adhesion to the epoxy resin matrix

HSIEN-TANG CHIU, JENG-SHYONG LIN
Research Program for Polymers and Textiles, National Taiwan Institute of Technology, Taipei, Taiwan

A method of improving the interfacial bonding between carbon fibre and epoxy resin matrix is developed in the case of continuous electrochemical deposition (ECD) of polypyrrole on carbon fibres. The ECD-treated carbon fibres are characterized by electron spectroscopy for chemical analysis (ESCA), scanning electron microscope (SEM), porous structure analysis and wettability measurements. Furthermore, mechanical evaluation is used to assess the macro-interfacial bonding capability of carbon fibre/epoxy resin composites. It is shown that there is a good interfacial bonding between ECD-treated carbon fibres and the epoxy resin. On the other hand, we also postulate the structure of polypyrrole-coated fibre to explain the bonding mechanism of carbon fibre/epoxy resin composites.

1. Introduction

During recent years, the successful development of excellent performance fibres has raised the quality of composite materials. The composites fabricated by such reinforcing materials as carbon fibres, boron fibres, and kevlar fibres are the so-called advanced composite materials (ACMS). To enhance the performance of ACMS, studies on the improvement of fracture toughness and delamination are essential.

In addition, the behaviour of delamination in composites is concerned with the property of interfacial bonding between resin and fibre. Therefore, how to modify the fibre/resin interface becomes an interesting question.

Regarding the surface treatment of carbon fibre, a lot of research has been done [1–6]. It mainly deals with either dry or with wet oxidation treatment to make the surface structure of the carbon fibre oxidated and to activate its functional group for improving adhesion to the matrix resin. As far as oxidation is concerned, the tensile strength of the carbon fibre decreases drastically because of the corrosion in the treatment processes. On the other hand, Dujardin *et al.* [7, 8] use the pyrrole electrochemical polymerization technique for carbon fibre surface modification. As a result, they found that the elongation of the carbon fibre and the interlaminar shear strength (ILSS) of the carbon fibre/epoxy laminate are increased. However, there is no further explanation of the properties of the interfacial bonding between pyrrole and carbon fibre. So more detailed work about the microscopic interfacial bonding (such as the mechanism of bonding between carbon fibre/polypyrrole and polypyrrole/epoxy) and macroscopic interfacial properties (such as ILSS) should be undertaken.

Moreover, the surface properties of the treated carbon fibre are strongly related to the interfacial adhesion performance. Hopfgarten *et al.* [9–16], employ ESCA or Auger spectroscopy to study the surface properties of carbon fibre. They also employ X-ray photoelectron spectroscopy (XPS) measurements to discuss the surface chemical components and the chemical bonding state of ECD-treated carbon fibre.

In this report, the continuous ECD process is performed. In the ECD process, the carbon fibre is used as a working electrode for the electrochemical reaction and a titanium plate as the counter electrode. The electrochemical oxidation is performed in an aqueous solution which contains pyrrole (0.19 M) and a supporting electrolyte (0.019 M). We change the supporting electrolyte in the ECD process to obtain different doping species on the carbon fibre and we discuss the influence of doping species on the surface morphology of carbon fibre and the interfacial bonding properties of carbon/epoxy composites.

2. Experimental procedure

2.1. The continuous ECD treatment

Untreated carbon fibres supplied by Toray Co., (T-300 C) were prepared by heat treatment under 300 °C for three hours. The electrochemical oxidation was performed in an aqueous solution which contained pyrrole (0.19 M) and a supporting electrolyte (0.019 M). Titanium and carbon fibres were used as the counter and working electrodes, respectively. Three kinds of supporting electrolyte were used: P-toluenesulphonic acid monohydrate, tetra-n-butylammonium perchlorate, and tetraethylammonium tetrafluoroborate. All the depositions were carried out at room temperature

0022–2461/92 $03.00 + .12

(27 °C). The working potential was about 12 V with a current density of approximately 30 mAcm^{-2}. The treated carbon fibres were dried in air at 100 °C for half an hour. Fig. 1a shows the equipment developed for the continuous ECD process for carbon fibres. In Fig. 1a, A is a feed roller for the carbon fibre, B is a reaction bath, C is the oven for drying, D & E are the power supply, F is a guide roller for the carbon fibre, and G is a take-up roller for the carbon fibre. The time of treatment can be adjusted by adjusting the running speed of the carbon fibres. The arrangement of the electrodes in the reaction bath is illustrated in Fig. 1b.

On the other hand, the free-standing polypyrrole film is obtained by using titanium for both working and counter electrodes. These free-standing polypyrrole films are used to compare the surface morphology with that of the ECD-treated carbon fibres.

2.2. Measurements

2.2.1. Fibre-tensile tests

The mechanical properties of the coated fibres (rupture load, stress, and strain) were studied on a 10 mm long single fibre with a Universal Testing Machine equipped with an automatic recorder of the

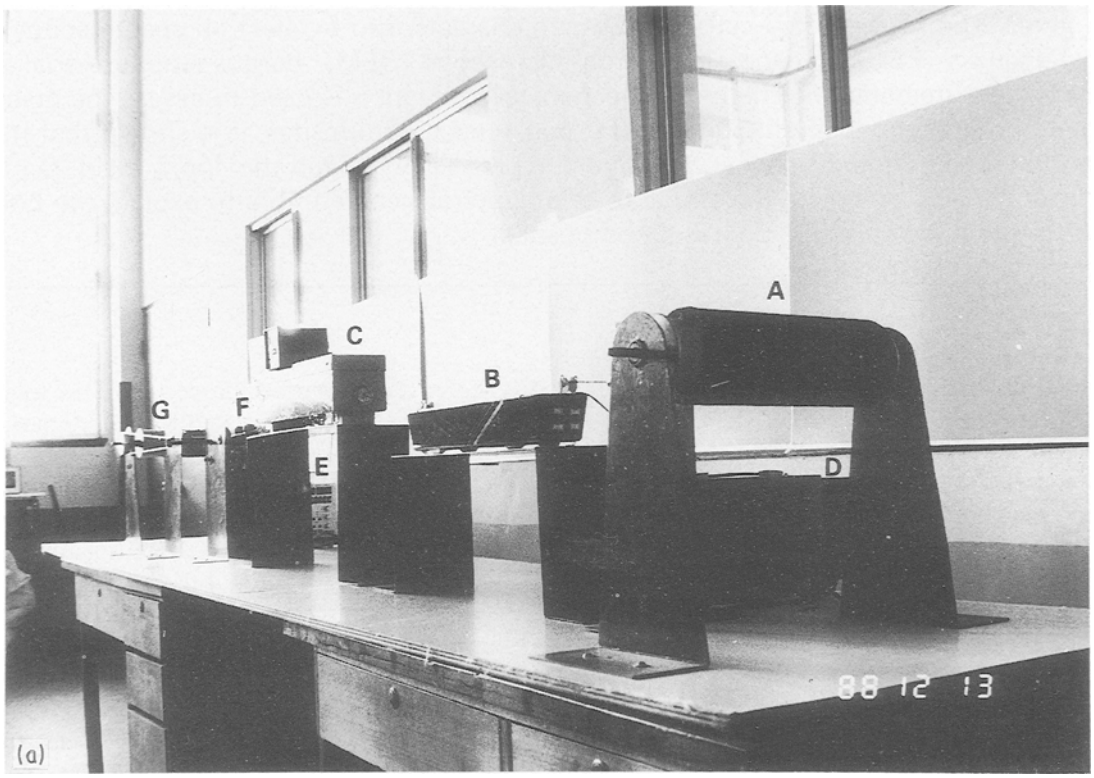

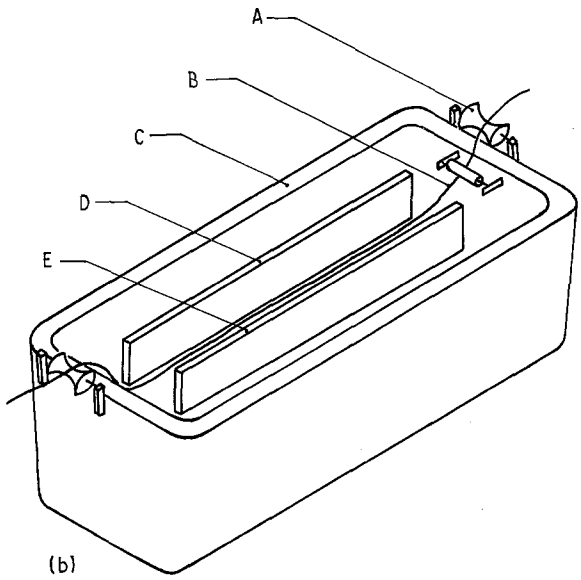

Figure 1(a) Continuous ECD process equipment. A: feed roller, B: reaction bath, C: oven, D: power supply, E: power supply, F: guide roller, G: take-up roller. (b) Continuous ECD process reaction bath equipment. A: guide roller, B: carbon fibres, C: reaction bath, D and E: titanium.

elongation–load curve, at a constant traction speed of 2 mm min^{-1}.

2.2.2. Contact angle tests

The wettability of carbon fibres was measured by a KYOWA contact angle meter MICRO-1. There were several approaches to measuring the contact angle in this test: of these, the drop method and length measurement were chosen. Fig. 2 interprets the contact angle, θ, obtained from $\tan \theta_1 = (h/r)$, where r equals half the length of the base line, h is the height of the drop, and the contact angle, θ, is twice, θ_1.

2.2.3. Evaluation of interfacial adhesion by interlaminar shear strength (ILSS)

The evaluation of the interfacial adhesion between carbon fibres and epoxy resin was carried out by using the interlaminar shear strength of a composite which contained 55% by volume of the ECD-treated carbon fibre. According to the short beam method, the samples for the ILSS tests were laminated by unidirectional carbon fibre/epoxy prepreg, and the size of the ILSS test specimen was $28 \times 12.7 \times 2$ mm.

2.2.4. Surface morphology of carbon fibres

The surface morphology was observed by using a Cambridge stereoscan S4-10 scanning electron microscope (SEM), under 20 kV.

2.2.5. Porous structure analysis

The mercury intrusion porosimetry Autopore II 9220 is used to measure the porous structure of the carbon fibres.

This instrument is based on a simple physical phenomenon involving the equilibrated intrusion of a non-wetting, non-reactive liquid into a porous material at selected pressures. A sample is evacuated, immersed in mercury, and the mercury pressure on the sample is isostatically increased, which causes the mercury to intrude into the pores. The pore size intruded is inversely proportional to the applied pressure. This permits a direct measurement of pore size and volume and provides the basis for the calculation of much related information. A reverse process, extrusion, allows additional data to be acquired which provides characterization of pore complexity.

Pore diameter and volume data are obtained from the equilibrated pressures where mercury intrudes into a given size pore.

The inverse relationship between pore diameter and the pressure is called the Washburn equation. It may be written

$$D = \frac{-4\gamma \cos\theta}{P} \quad (1)$$

where D is pore diameter when P is the applied pressure.

The surface tension (γ) and the interfacial contact angle (θ) of the mercury are assumed to remain unchanged during the intrusion or extrusion segment of the analysis. For routine calculation, $\gamma = 485$ dynes/cm and $\theta = 130°$ are normally used. For ultimate accuracy, the correct contact angle between the mercury and the solid sample surface must be determined, for example, by using a Micromeritics contact anglometer.

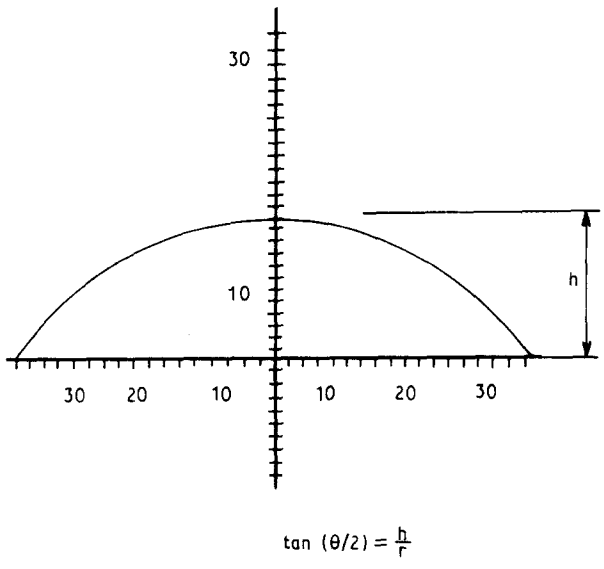

Figure 2 The measurement of contact angle by drop method.

2.2.6. X-ray photoelectron spectroscopic analysis

The XPS spectra analysis was carried out on a Perkin Elmer PHI 1905 X-ray photoelectron spectrometer, under $5 \times 10^{-9} \sim 10^{-10}$ torr vacuum conditions.

3. Results and discussion

3.1. Morphology and bonding model of polypyrrole on carbon fibres

Figs 3 and 4 are the SEM surface photographs which show the profile and cross sectional views of ECD-treated carbon fibres. Comparing the SEM results with untreated carbon fibres, we can recognize the coating of polypyrrole on the carbon fibres.

The oxidation reaction of polypyrrole on the carbon fibre anode has been recognized by Tooru and Toshihiro [17]. Using carbon fibre as the anode can produce a polypyrrole coating on the carbon fibre through an oxidation reaction and form a structure of coating film.

The formation of the polypyrrole film on the carbon fibre is schematically illustrated by Fig. 5. Initially, the radical cation is formed by a redox reaction; then it dimerizes to the adduct having the structure of a dication, which stabilizes itself by deprotonation to give the stable dimer of pyrrole. By continuing the process of oxidation of the dimer and deprotonation, it deposits a layer of polypyrrole film on the carbon fibre in order to ameliorate the nature of its surface [20].

In the ECD process, various supporting electrolytes can lead to a myriad of results. At the moment of

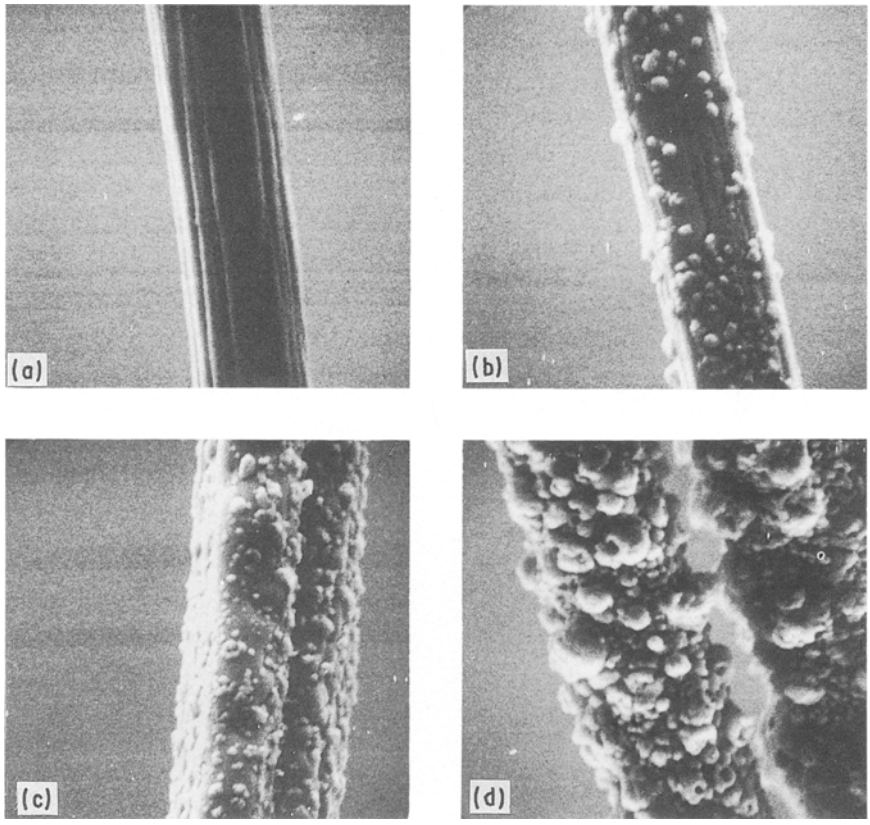

Figure 3 Scanning electron micrographs of polypyrrole-coated carbon fibres prepared by using different electrolytes (a) Virgin (b) $CH_3C_6H_4SO_3H \cdot H_2O$ (c) $(C_2H_5)_4NBF_4$ (d) $(C_4H_9)_4NClO_4$.

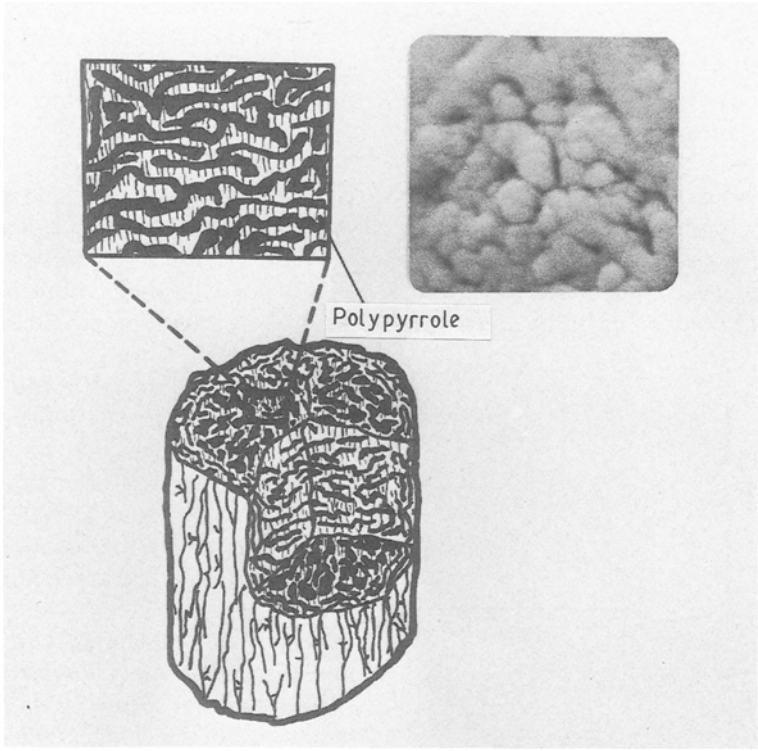

Figure 4 Postulated model for polypyrrole on carbon fibre and SEM cross-sectional photograph of ECD-treated carbon fibre.

anode oxidation, the electrolyte charged with anions will dope to form pyrrole$^+$–X$^-$ complex.

According to the doping species of polypyrrole, the general chemical structure of the deposition layer on the carbon fibres is shown in Fig. 6.

On the other hand, many reports show that the carbon fibres possess a porous microstructure [21–26]. During the ECD process for carbon fibres, the reaction of the polypyrrole deposits it in molecular order on the carbon fibre and then it grows as a film

layer. Since the polypyrrole not only deposits a polypyrrole film on the carbon fibre surface, but also enters the void constitution of the carbon fibre, we can get a strong bonding between the ECD-treated polypyrrole film and the carbon fibre.

This phenomenon can be verified by the SEM cross-sectional view of ECD-treated carbon fibre shown in Fig. 4.

Comparing how the different ECD treatments affect the surface morphology, we discover that the different electrolytes result in clearly different sizes of polypyrrole grains. From Figs 3–4, we find that doping with SO_3H^- results in larger surface grains while the sample doped with BF_4^- has smaller grains, but the sample doped with ClO_4^- has uniform grains and a higher density surface. For comparing the surface morphology of polypyrrole, the SEM profiles of free-standing polypyrrole film are shown in Fig. 7. The results are the same as those observed with the polypyrrole on carbon fibres.

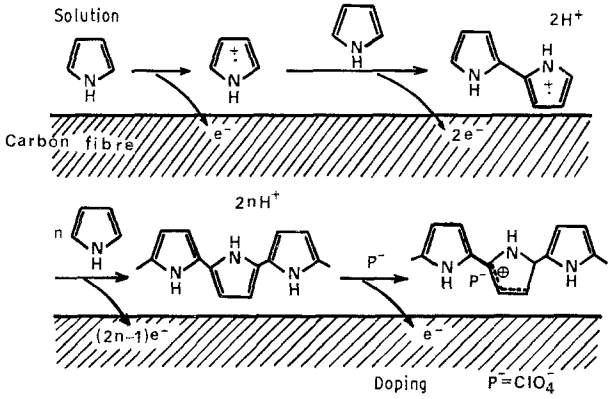

Figure 5 The reaction model for polypyrrole on carbon fibre.

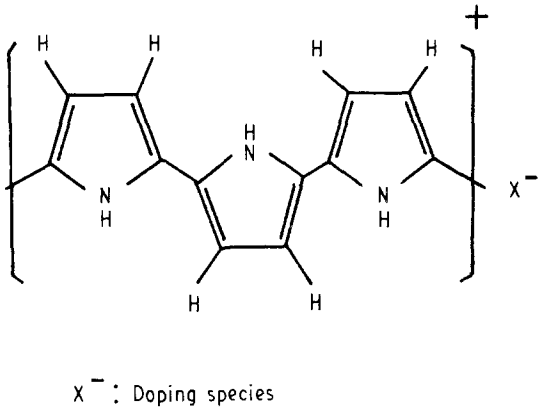

Figure 6 A possible structure of polypyrrole.

3.2. Pore structure analysis of carbon fibre

In the above discussion, we assumed that the polypyrrole molecules are deposited from the inner surface to the outer surface of the carbon fibre during the ECD process. Since the polypyrrole molecules enter the core structure of the carbon fibre, they can provide a good cohesion force between the carbon fibre and the polypyrrole at the interface.

This phenomenon can also be examined using the porous structure analysis technique. Fig. 8a–8d shows the information on the pore size distribution of the carbon fibres. We find that the pore size distribution of the carbon fibres ranging from 1–100 μm has changed significantly. This means that polypyrrole molecules penetrate precisely into the core void structure of the carbon fibre, which causes the larger void to form new smaller void structures. From the SEM and porous analysis results, the deposition process and the adhesion of polypyrrole on the carbon fibres can be clearly observed.

3.3. Mechanical properties of polypyrrole-coated carbon fibres

Table I shows the stress/strain behaviour of ECD-treated single fibres. Obviously, the stress at the break

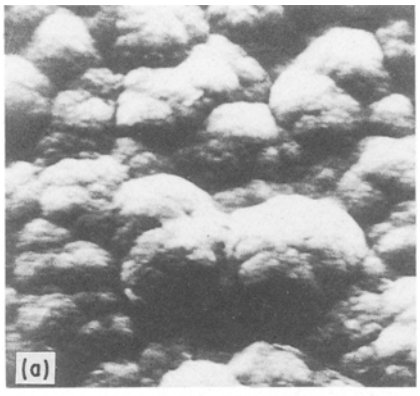

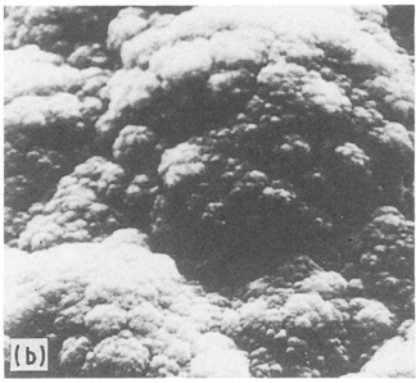

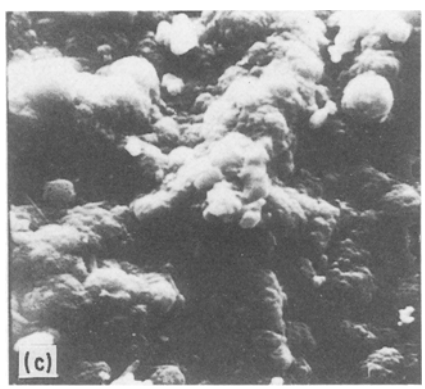

Figure 7 Scanning electron micrographs of polypyrrole films prepared by using different electrolytes (a) $CH_3C_6H_4SO_3H \cdot H_2O$ (b) $(C_2H_5)_4NBF_4$ (c) $(C_4H_9)_4NClO_4$.

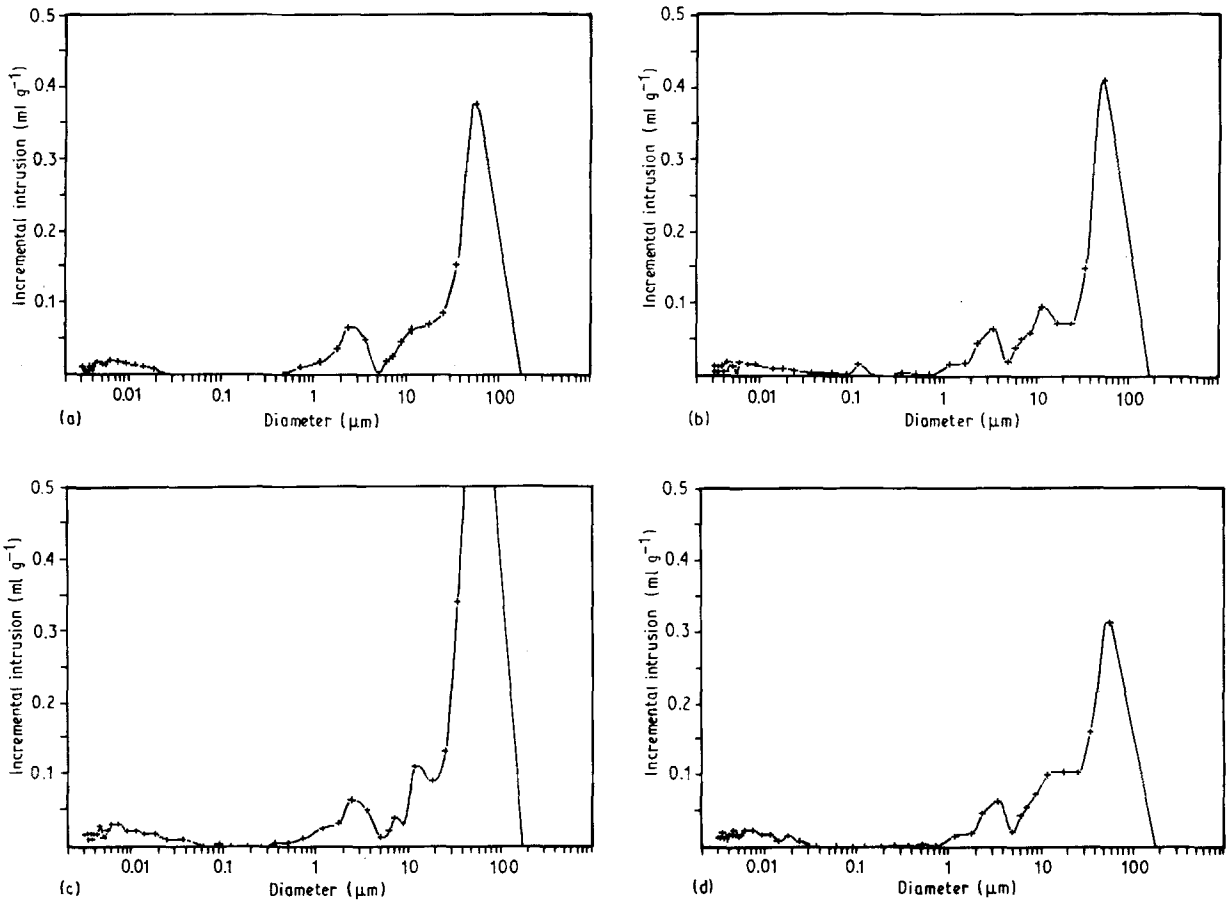

Figure 8 Pore size distribution of (a) untreated carbon fibres, (b) polypyrrole-coated carbon fibres prepared by using $CH_3C_6H_4SO_3H \cdot H_2O$ electrolyte, (c) polypyrrole-coated carbon fibres prepared by using $(C_2H_5)_4NBF_4$ electrolyte and (d) polypyrrole-coated carbon fibres prepared by using $(C_4H_9)_4NClO_4$ electrolyte.

TABLE I Effect of polypyrrole treatment on tensile properties of carbon fibres.

Supporting electrolyte	Cross-section (cm^2) $\times 10^{-7}$	Tensile strength (MPa)	Elongation (%)
Virgin	7.85	3400	1.4
Heat treatment	7.67	3390	1.38
$CH_3C_6H_4SO_3H \cdot H_2O$	9.09	3313	1.62
$(C_2H_5)_4NBF_4$	10.21	3340	1.73
$(C_4H_9)_4NClO_4$	10.40	3385	1.81

in the specimens decreases with the electrochemical polymerization treatment, and the elongation at the break increases.

Obviously, the counter anions incorporated from the supporting electrolyte solutions have been shown to influence the tensile properties of polypyrrole-coated fibres. We assume that the anion species of the supporting electrolytes profoundly influence the morphologies of the resulting polypyrroles. Electron microscopy clearly reveals the existence of surface modifications, typical SEM data being shown in Figs 3–4. The mechanical properties of ECD-treated carbon fibres include conjugate fibre behaviour. Since the elastic modulus of the polypyrrole film is lower than that of the carbon fibre, a toughening effect is observed in any ECD-treated carbon fibres.

TABLE II Effect of doping species on contact angle.

Doping species	r	h	θ
Virgin	17.2	15.5	83.8
$CH_3C_6H_4SO_3H \cdot H_2O$	14.2	12.3	81.9
$(C_2H_5)_4NBF_4$	13.4	11.5	81.6
$(C_4H_9)_4NClO_4$	14.3	12.2	81.1

3.4. The wettability of polypyrrole-coated carbon fibres

The wettability of solids (carbon fibre, metal, glass, etc.) on which a drop acts is dependent on the intermolecular attractive force. If this force between liquid and solid is strong enough, the wettability obtained from the contact angle (θ) should be prominent ($\theta = 0°$). If the attractive force between liquid and solid is weaker than that between liquid and liquid, then the wettability of the drop to the solid is lower ($\theta \ll 90°$) than that to the liquid. So, we have defined $\theta \gg 90°$ as hydrophobic.

The test value of the contact angle of polypyrrole-coated carbon fibres prepared by using different electrolytes and solvents is shown in Fig. 9 and Table II. It is measured by a KYOWA contact angle meter MICRO-1. We find that the surface modification by polypyrrole on the carbon fibre causes the contact angle (θ) to decrease. The decrease of the contact angle by ECD treatment suggests that, through surface

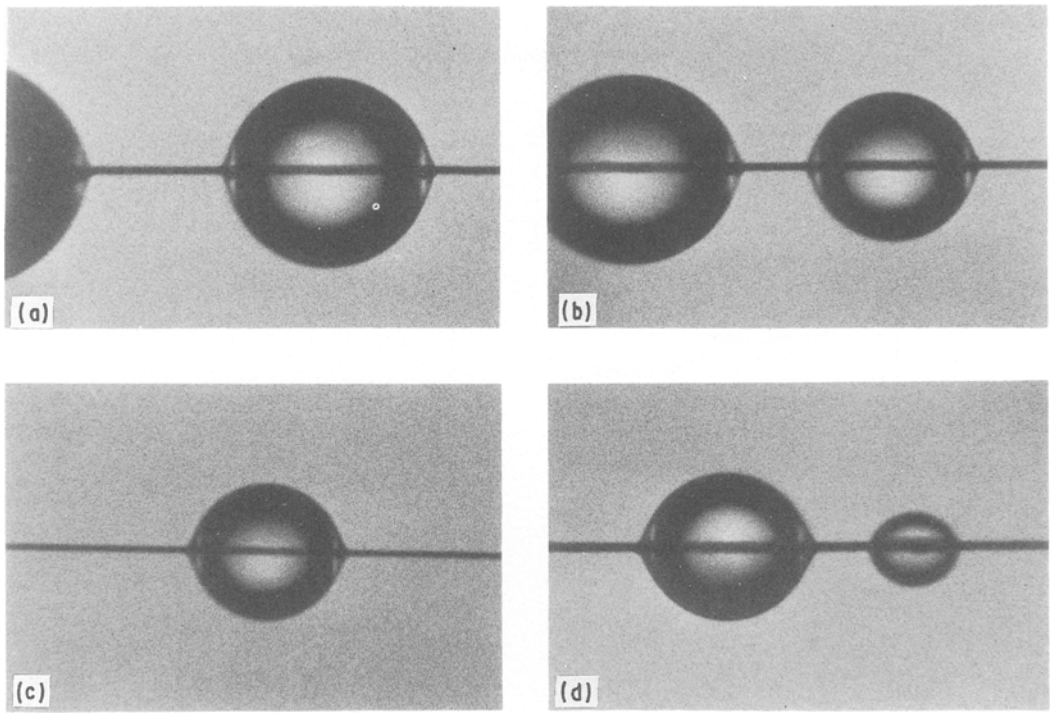

Figure 9 Contact angle of polypyrrole-coated carbon fibres prepared by using different electrolytes for (a) Virgin, (b) $CH_3C_6H_4SO_3H \cdot H_2O$ (c) $(C_2H_5)_4NBF_4$ and (d) $(C_4H_9)_4NClO_4$.

modification by the polypyrrole, the carbon fibre becomes more accessible to the epoxy resin matrix. This wetting accessibility depends on the doping species, due to its affect on the surface morphology of the carbon fibre.

3.5. Interlaminar shear strength of carbon fibre/epoxy composites

The data presented in Table III show that polypyrrole treatments are capable of enhancing strongly the bond strength of carbon/epoxy laminates. The shear strength (σ_s) is defined by

$$\sigma_s = \frac{3P}{4b\bar{d}} \quad (2)$$

where P designates ultimate bending strength, and b and d indicate the width and thickness of the specimen, respectively.

As shown in Table III, the shear strength of polypyrrole-coated carbon fibres is dependent on the doped anion species in the polypyrrole films. We find that the ILSS of ECD-treated carbon fibre/epoxy laminates has evidently increased. As far as the effect of polypyrrole treatment on ILSS is concerned, two main principles have to be taken into consideration. The first is the facilitation of chemical bonding between the fibre and the matrix by forming a resin-compatible fibre surface through the interaction between doped anion and matrix. The second principle is the surface roughness of the polypyrrole films, which form the mechanical interlocking between fibre and resin matrix. Fig. 4 shows the SEM profiles of polypyrrole films prepared by using different electrolytes. We find that the surface of ClO_4^- doped polypyrrole film is more compact and rougher than that resulting from other doping species. This effect reveals that the surface morphology of carbon fibre is one dominant factor in ILSS performance and, through the ECD process, we can control the surface morphology of carbon fibres by selecting the doping species of the polypyrrole. In this research we have improved the ILSS, which increases about 47% by using the ClO_4^- doping species in the ECD process.

TABLE III Interlaminar shear strength of carbon fibre/epoxy laminates.

Anion species	Shear strength (MPa)
Virgin	70.9
$CH_3C_6H_4SO_3H \cdot H_2O$	93.8
$(C_2H_5)_4NBF_4$	100.1
$(C_4H_9)_4NClO_4$	104.4

3.6. ESCA spectra of polypyrrole-coated carbon fibres

The ESCA spectra provide useful information on the levels and nature of oxidation in the carbon fibres before and after the various pretreatments.

Fig. 10a shows the spectrum of untreated carbon fibres. The intensity of the O_{1s} signal comes from the oxidative surface treatment which tends to increase the chemical reactivity of the fibre by creating hydroxyl, carbonyl and carboxyl groups. After ECD treatment, we detect the S_{1s}, F_{1s} and Cl_{1s} lines, the peaks of which correspond to the presence of the electrolyte anion (SO_3H^-, BF_4^-, ClO_4^- in this case) introduced into the film during the growth of the polymer in Fig. 10b–d. The chemical composition within the fibre subsurface shown by the ESCA technique is sufficiently accurate. The core-level binding energies of

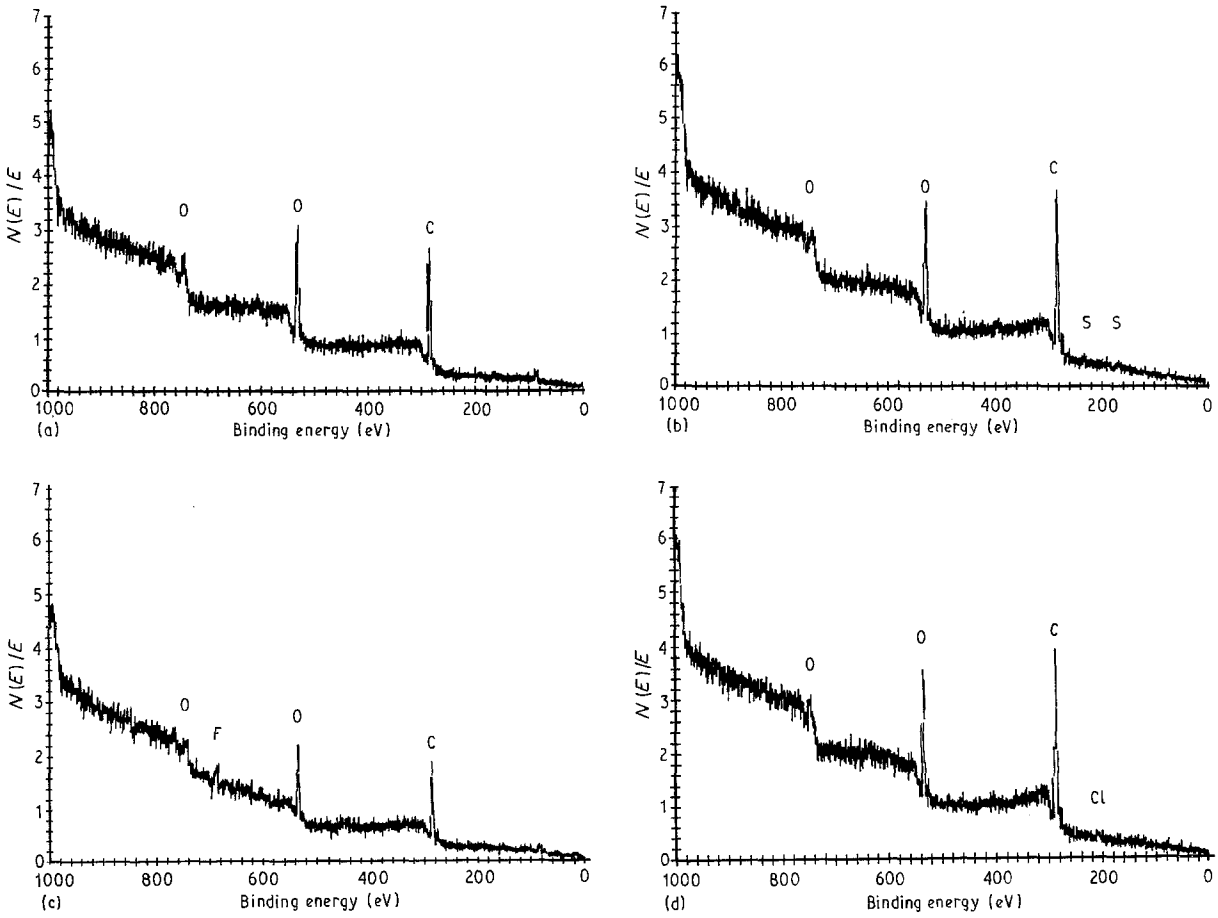

Figure 10 ESCA spectra of (a) untreated carbon fibres (b) polypyrrole-coated carbon fibres prepared by using $CH_3C_6H_4SO_3H \cdot H_2O$ electrolyte) (c) polypyrrole-coated carbon fibres prepared by using $(C_2H_5)_4NBF_4$ electrolyte and (d) polypyrrole-coated carbon fibres prepared by using $(C_4H_9)_4NClO_4$ electrolyte.

TABLE IV XPS core-level binding energies of polypyrrole on fibres (eV).

Anion species	C_{1s}	O_{1s}	S_{1s}	F_{1s}	Cl_{1s}
Virgin	284.4	532.2			
$CH_3C_6H_4SO_3H \cdot H_2O$	284.8	532.2	168		
$(C_2H_5)_4NBF_4$	284.2	531.8		685.6	
$(C_4H_9)_4NClO_4$	285	532.6			208.4

polypyrrole synthesized on carbon fibres are listed in Table IV. The chemical shift of C_{1s} and O_{1s} with the ClO_4^- doping species is larger than with other doping species. This result combined with the ILSS information suggests that some chemical interactions contribute to the interfacial bonding properties.

4. Conclusions

In this paper, we have shown that the ECD treatment produces a significant effect on the interfacial bonding of carbon/epoxy composites. We also suggest a structural model for polypyrrole on carbon fibres and the relationship between the ECD process and interfacial properties. The conclusions of this work can be summarized as follows:

(i) The continuous ECD process for surface modification of carbon fibre is a convenient and useful technique. The thickness of the modification layer depends on the processing speed, which can be varied by varying the working potential and the working time during the ECD treatment.

(ii) From the cross-sectional view of SEM and porous structure analysis, we postulate a structural model for polypyrrole-coated carbon fibre. Since the polypyrrole molecules deposit from the internal surface to the outer surface of the carbon fibre, we can get a strong cohesion force between the carbon fibre and polypyrrole.

(iii) The increase in the ILSS of carbon fibre/epoxy composites depends on the doping species used in the ECD process. Using SEM and wettability examination, we consider that the effect on ILSS is due to the surface morphology of the polypyrrole layer on the carbon fibre.

(iv) XPS analysis confirms the composition of polypyrrole. We also find that the modification layer of polypyrrole can provide a surface activation of the carbon fibre to improve the interfacial performance of carbon/epoxy composites.

Acknowledgement

We thank the National Science Council of Taiwan for support for this work under the project NSC 77-0405-E011-12.

References

1. FUJISAWA, A. TANAKA, K. HASHIMOTO, and M. KOBAYASHI, *A. C. S. Polym. Preprints* **20** (1979) 853.
2. J. J. BRENNAN, T. E. JERMYN, and B. BOONSTRA, *J. of Appl. Polym. Sci.* **8** (1964) 2687.
3. J. L. KARDOS, F. S. CHENG, and T. L. TOLBERT, *Polym. Eng. and Sci* **13** (1973) 455.
4. R. J. DAUKSYS, *A. F. M. L.* (1972) 22–23.
5. N. J. DELOLLIS, *Sample J.* **15** (1979) 10.
6. R. V. SUBRAMANIAN, and J. J. JUKUBOWSKI, *Polym. Eng. and Sci.* **18** (1978) 590.
7. S. DUJARDIN, J. BOUTIGUE, C. M. DESBUGUOIT, J. RIGA, and J. VERBIST, *Mol. Cryst. Lig. Cryst.* **118** (1985) 249.
8. S. DUJARDIN, R. LAZZARONI, L. RIGO, J. RIGA, and J. VERBIST, *J. Mater. Sci.* **21** (1986) 4342.
9. F. HOPFGARTEN, *Fibre Sci. and Tech.* **11** (1978) 67.
10. *Idem, ibid.* **12** (1979) 283.
11. D. M. BREWIS, J. COMYN, J. R. FOWLER, D. BRIGGS, and V. A. GIBSON, *ibid.* **12** (1979) 41.
12. K. WALTERSSON, *ibid.* **17** (1982) 289.
13. *Idem, Compos. Sci. and Tech.* **22** (1985) 223.
14. *Idem, ibid.* **23** (1985) 303.
15. D. YOUXIAN, W. DIANXUM, S. MUJIN, C. CHUANZHENG, and Y. JIN, *ibid.* **30** (1987) 119.
16. M. TAKAYAGI, T. KATAYOSE, T. KAGIYAMA, *J. Appl. Polym. Sci.* **27** (1982) 3903.
17. I. TOORU, and Y. TOSHIHIRO, *Bull. Chem. Soc. Japan.* **56** (1983) 985.
18. E. M. GENIES, G. BIDAN, and A. F. DIAZ, *J. Electroanal. Chem.* **149** (1983) 101.
19. K. S. V. SANTHANAM, *ibid.* **160** (1984) 377.
20. G. WEGNER, *Angew. Chem. Int. Ed. Engl.* **20** (1981) 361.
21. D. J. JOHNSON, and C. N. TYSON, *Brit. J. Appl. Phys. (J. Phys. D.)* **2** (1969) 787.
22. D. J. JOHNSON, D. CRAWFORD, and C. OATES, 10th Bien. Carbon Conf., Bethlehem. PA. (1971) p. 29.
23. A. FOURDEUX, R. PERRET, and W. RULAND, Proc. 1st Int. Conf. Carbon Fibres, London (1971) p. 57.
24. F. R. BARNET, and M. K. NOOR, Proc. 2nd Int. Conf. Carbon Fibres, London, Plastics Institute (1974) p. 32.
25. A. OBERLIN, 15th Carbon Conf., Philadelphia (1981) p. 288.
26. M. GUIGON, A. OBERLIN, and G. DESARMOT, *Fibre Sci. and Tech.* **20** (1984) 177.

Received 22 January
and accepted 6 November 1990